

# Journal of Materials Chemistry A

Accepted Manuscript



This is an *Accepted Manuscript*, which has been through the Royal Society of Chemistry peer review process and has been accepted for publication.

*Accepted Manuscripts* are published online shortly after acceptance, before technical editing, formatting and proof reading. Using this free service, authors can make their results available to the community, in citable form, before we publish the edited article. We will replace this *Accepted Manuscript* with the edited and formatted *Advance Article* as soon as it is available.

You can find more information about *Accepted Manuscripts* in the [Information for Authors](#).

Please note that technical editing may introduce minor changes to the text and/or graphics, which may alter content. The journal's standard [Terms & Conditions](#) and the [Ethical guidelines](#) still apply. In no event shall the Royal Society of Chemistry be held responsible for any errors or omissions in this *Accepted Manuscript* or any consequences arising from the use of any information it contains.

**Innovative high performing metal organic framework (MOF)-laden nanocomposite polymer electrolytes for all-solid-state lithium batteries**

Claudio Gerbaldi<sup>1,\*</sup>, Jijeesh R. Nair<sup>1,\*</sup>, M. Anbu Kulandainathan<sup>2</sup>, R. Senthil Kumar<sup>2</sup>, Chiara Ferrara<sup>3</sup>, Piercarlo Mustarelli<sup>3</sup> and Arul Manuel Stephan<sup>2,\*</sup>

1) *GAME Lab, Department of Applied Science and Technology – DISAT, Institute of Chemistry, Politecnico di Torino, C.so Duca degli Abruzzi 24, 10129 Torino, Italy.*

2) *Central Electrochemical Research Institute (CSIR-CECRI), Karaikudi 630 006, India.*

3) *Department of Chemistry, Section of Physical Chemistry, University of Pavia, and INSTM, Via Taramelli 16, Pavia, Italy*

\* Corresponding authors: Claudio Gerbaldi, Jijeesh R. Nair ([claudio.gerbaldi@polito.it](mailto:claudio.gerbaldi@polito.it), [jijeesh.nair@polito.it](mailto:jijeesh.nair@polito.it); PHONE: +39 011 090 4643; FAX: +39 011 090 4699; contact details: affiliation 1) and Arul Manuel Stephan ([arulmanuel@gmail.com](mailto:arulmanuel@gmail.com); PHONE: +91 4565 241426; FAX: +91 4565 227779; contact details: affiliation 2).

**Abstract**

Two orders of magnitude enhancement in the ambient temperature ionic conductivity of poly(ethylene oxide)-based nanocomposite polymer electrolyte (NCPE) membranes is here fundamentally achieved by the incorporation of specific amounts of aluminium-based metal organic framework (MOF) as the filler. Thorough characterisation, particularly, solid-state NMR and FT-IR studies, shed light on the specific role of the defective MOF frameworks in greatly enhancing the Li<sup>+</sup> ions mobility inside the polymeric matrix. The prepared NCPEs are highly stable towards lithium metal even after prolonged storage time and an excellent cycling profile is evidenced even at moderate temperature which has never been reported so far for an all solid state lithium polymer cell composed of Li/NCPE/LiFePO<sub>4</sub>.

**Keywords:** metal organic framework, poly-ethylene oxide, polymer electrolyte, ionic conductivity, lithium battery

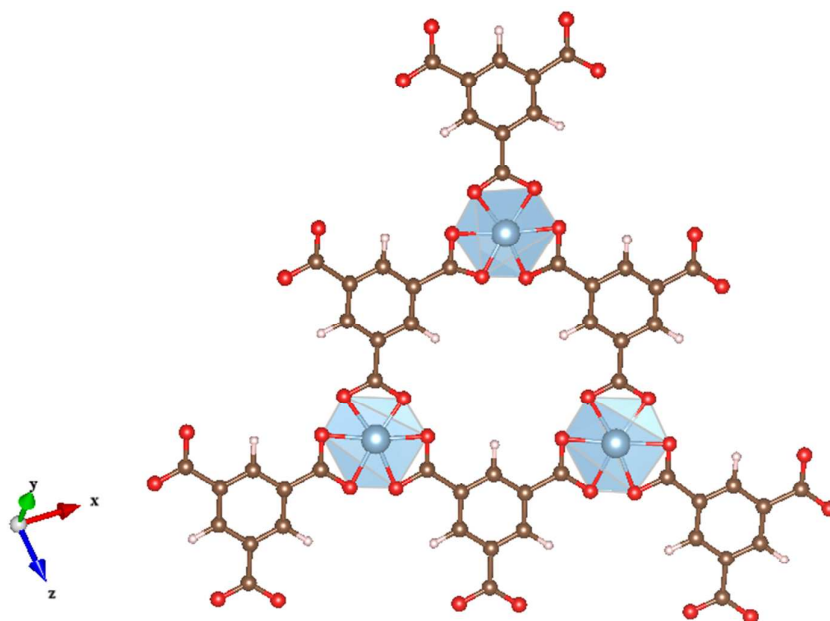
The unique properties such as high single cell working potential, energy density, long cycle life, etc., have identified secondary Li-ion batteries as the power source of choice for portable electronic devices such as laptop computers, cellular phones, digital cameras, etc.<sup>1</sup> However, their possible widespread penetration into the hybrid electric vehicle (HEV) and plug-in HEV large-scale markets may be realized only when substantial improvements such as low cost, sustainability, safety, high rate capability and long calendar life are achieved.<sup>2,3</sup>

The advancement in lithium battery technology relies mainly upon replacement of the conventional liquid electrolyte by an advanced solid polymer electrolyte. In order to achieve this goal, many lithium-conducting polymeric networks have been prepared and characterized over the years.<sup>4</sup> Among the polymer hosts explored so far, poly(ethylene oxide) - PEO has been indeed the most extensively studied system.<sup>5</sup> Unfortunately, solid polymer electrolytes comprising such a polymer host and a lithium salt (e.g., PEO + LiClO<sub>4</sub>) exhibit insufficient ionic conductivity at ambient and sub-ambient temperatures.<sup>6</sup> Indeed, despite its several advantages such as low cost, good chemical stability and safety, PEO exhibits appreciable ionic conductivity only above 70 °C which excludes it from ambient temperature applications.<sup>1</sup> Numerous attempts have been made to enhance the ionic conductivity of PEO-based electrolytes; one of the most common ways is the addition of low molecular weight liquid plasticizers like ethylene carbonate, propylene carbonate, etc. Although it ameliorates the ionic conductivity, the addition of plasticizers adversely deteriorates both mechanical integrity and safety of the electrolyte membrane; moreover, side reactions with lithium metal eventually occur. In a pioneering research, Weston and Steele incorporated  $\alpha$ -alumina as filler in a poly(ethylene oxide) matrix, observing an increase in the ionic conductivity of the composite system.<sup>7</sup> Scrosati and coworkers demonstrated that the addition of filler acts as a solid plasticizer in

the PEO matrix, thus inhibiting the chain reorganization.<sup>8</sup> This reorganization stabilizes the amorphous phase at lower temperature, which provides a useful range of electrolyte conductivity. The degree of reorganization depends upon the nature of the inert filler used. Dispersion of nano-sized ceramic fillers, such as TiO<sub>2</sub>, Al<sub>2</sub>O<sub>3</sub> and SiO<sub>2</sub> in the polymeric matrix significantly improved the ionic mobility in the polymeric matrix.<sup>9</sup> By the addition of sulphate-promoted super acid zirconia (S-ZrO<sub>2</sub>) ceramic filler, a very high lithium transference number ( $T_{Li^+} = 0.81 \pm 0.05$ ) has also been obtained, which is nearly double the value of the ceramic-free electrolyte ( $0.42 \pm 0.05$ ).<sup>10</sup> The increased transport number value was attributed to the Lewis acid-base interactions occurring between the surface of the ceramic filler and both the X<sup>-</sup> anion of the salt and the segments of the PEO chain. In an unconventional way of thinking, Bruce et al. illustrated the ionic conductivity in the crystalline complexes of PEO+LiXF<sub>6</sub> (where X = P, As, Sb).<sup>11</sup> Recently, new interesting structures have been described in the literature, namely metal organic frameworks (MOFs).<sup>12</sup> Generally speaking, they are microporous solids consisting of an infinite network of metal centres (or inorganic clusters) bridged by simple organic linkers through metal–ligand coordination bonds.<sup>13</sup> MOFs are widely used in catalysis, sensors, ion exchange, gas storage, purification, separation and sequestration;<sup>14</sup> they are also used in optoelectronics to improve both electronic and proton conductivity.<sup>14f</sup> Recently, Wiers and co-workers demonstrated an increase in ionic conductivity of a solid electrolyte by adding lithium isopropoxide to a Mg-based metal organic framework followed by soaking in a conventional liquid electrolyte.<sup>15</sup> In a similar way, Yuan et al. proposed a Zn-based MOF-5 as novel filler for PEO-based nanocomposite polymer electrolytes showing improved electrochemical properties in Li-ion cells.<sup>16</sup> Nevertheless, to the best of our knowledge, so far no attempt has been made on the development of PEO-based nanocomposite polymer electrolytes (NCPEs) encompassing an ad hoc synthesized Al-BTC (aluminium benzenetricarboxylate) MOF and a proper lithium salt showing an enhanced ionic conductivity of more than two orders of magnitude at low temperature and excellent stability towards lithium metal even after a prolonged period of storage. The obtained metal organic

frameworks and macromolecular nanocomposite networks are thoroughly characterized from the structural, morphological and physico-chemical viewpoint and, for the first time, an excellent long-term electrochemical behaviour in a lab-scale  $\text{LiFePO}_4/\text{NCPE}/\text{Li}$  cell is demonstrated (noteworthy stable even at low  $50\text{ }^\circ\text{C}$ ), thus accounting for the development of high performing, safe all-solid-state lithium cells. Even though plenty of literature data are available on ceramic based fillers, the studies based on polymer electrolytes encompassing MOFs are truly interesting due to their tailor-making capability and the broad spectrum of opportunities and possibilities it can bring. If very well-tuned, MOF-based fillers would become a true promising candidate and a vital ingredient which can enforce the intrusion of polymer electrolytes into the huge market of lithium-based batteries conceived for moderately low temperature applications.

Al-BTC MOF was synthesized by an electrolytic process and its proposed ideal structure is schematised in **Scheme 1**. Details of the preparation procedure and characterization of the MOF powder are extensively presented and thoroughly discussed in Supporting Information (S.I.).



**Scheme 1** Schematic diagram representing the ideal network structure of aluminium(III)-1,3,5-benzenetricarboxylate (namely, Al-BTC) metal organic framework.

For the preparation of the all-solid-state nanocomposite polymer electrolytes, poly ethylene oxide (PEO, Aldrich, USA) and lithium bis(trifluoromethanesulfonimide) -  $\text{LiN}(\text{CF}_3\text{SO}_2)_2$  (LiTFSI, Merck, Germany) were dried under vacuum for 2 days at 50 and 100 °C, respectively, before use. Al-BTC was also dried under vacuum at 50 °C for 5 days before use. Nanocomposite polymer electrolytes (NCPEs) were prepared by dispersing appropriate amounts of Al-BTC in the PEO - LiTFSI mixture (see Table 1 for the list and compositions of samples prepared) and hot-pressing into films as detailed elsewhere.<sup>17</sup> The complete dispersion was achieved by mechanical mixing with Ultra-Turrax<sup>®</sup> for 3 min. NCPE films had an average thickness of  $30 \pm 10$   $\mu\text{m}$ . This procedure yielded homogeneous and mechanically abusable membranes, which were dried under vacuum at 50 °C for 24 h for further characterization. Five different nanocomposite polymer electrolyte membranes encompassing Al-BTC metal organic frameworks were prepared, having varying amounts of PEO, Al-BTC and LiTFSI salt, respectively, as shown in **Table 1**.

**Table 1.** List of the samples prepared along with their compositions expressed in weight percent (wt.%) of the total weight.

| Sample | PEO | Al-BTC MOF | LiTFSI |
|--------|-----|------------|--------|
| S1     | 95  | 0          | 5      |
| S2     | 93  | 2          | 5      |
| S3     | 85  | 10         | 5      |
| S4     | 80  | 10         | 10     |
| S5     | 75  | 10         | 15     |

Differential Scanning Calorimetry (DSC) measurements were carried out in order to identify the extent of intercalation and exfoliation of the fillers in the NCPEs. **Figure 1** shows the DSC thermograms of the nanocomposite polymer electrolytes measured from -100 to +100 °C. The melting point of the PEO + LiTFSI electrolyte is increased from 59 to 66 °C upon addition of MOF in the polymeric system. Similarly, the glass transition temperature ( $T_g$ ) is also increased from -54 to -48 °C. The  $T_g$  increase of the NCPE with respect to the PEO might be due to: (i) the effect of a small amount of dispersed particles, and (ii) confinement of the intercalated/exfoliated polymer

chains within the filler galleries, which resists the segmental motion of the polymer chains.<sup>18</sup> In particular, the increase in the  $T_g$  value of NCPEs (towards the positive side) indicates better polymer–filler interaction, while the decrease in  $T_g$  (towards the negative side) accounts for the plasticization effect. The marginal decrease in the melting point of the PEO polymer at higher concentration of fillers is attributed to the mild retarding effect on the crystallization that arises because of the added filler/MOF particles.<sup>19</sup>

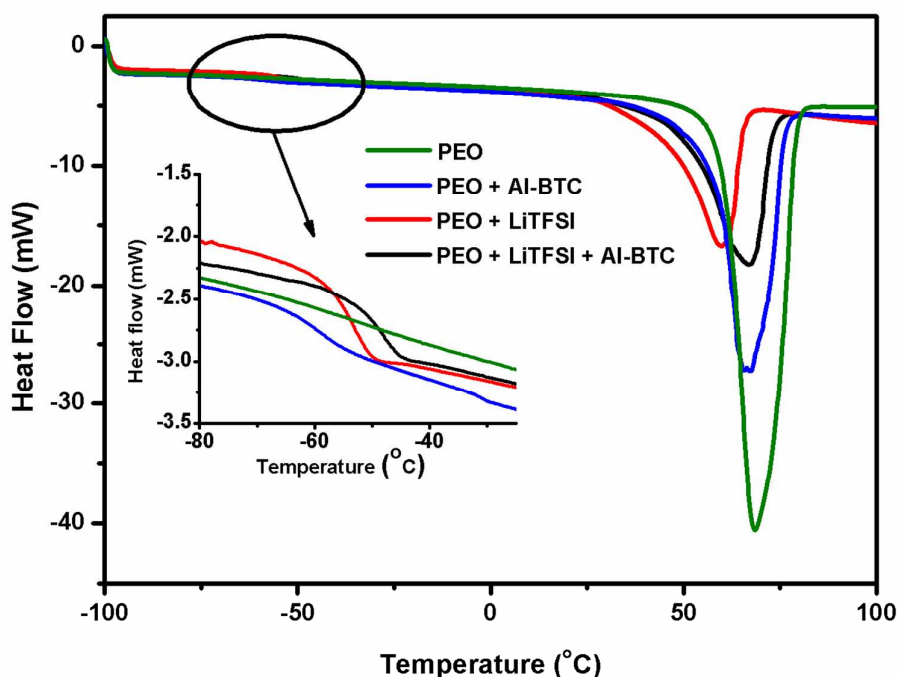


**Fig. 1** DSC traces of PEO, PEO+Al-BTC, PEO+LiTFSI and the nanocomposite polymer electrolyte PEO+LiTFSI+Al-BTC.

The thermo-gravimetric, both TGA in red and DTA in blue, traces of PEO+LiTFSI+Al-BTC(MOF) (viz sample S4) are depicted in **Figure 2**. The endothermic peak that appears around 70 °C is due to the melting of the crystalline PEO.<sup>20,21,22</sup> No further appreciable weight losses are observed until the irreversible decomposition which starts at around 345 °C. This confirms that the nanocomposite polymer electrolyte membrane can be safely used at fairly higher temperatures than the normal operating temperature of lithium batteries, at least in nitrogen atmosphere. The increase in the thermal stability of the nanocomposite polymeric membrane is attributed to the

intercalation/exfoliation of the polymer matrix with inert particles, which results in a strong barrier effect preventing to a certain extent from the thermal degradation.<sup>22</sup>

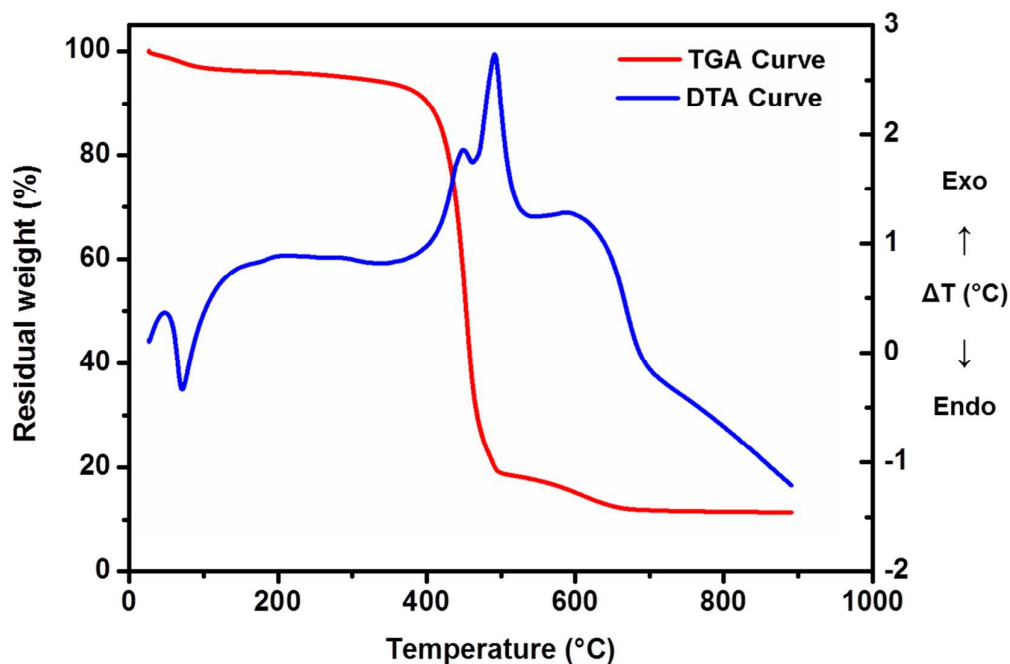


**Fig. 2** Thermo-gravimetric analysis, under  $N_2$  flow in the temperature range 25–900 °C, of sample S4.

In order to employ the newly elaborated macromolecular nanocomposites in all-solid-state lithium polymer batteries, the ionic conductivity was measured for the samples prepared with various concentrations of PEO, LiTFSI and Al-BTC MOF. In the present study, NCPEs were prepared by limiting the maximum concentration of lithium salt to 10-15 wt. %, in order to obtain the optimal compromise between high ionic conductivity, transport number and negligible unwanted reactions which can eventually limit the long-term cycling stability in real cell configuration.<sup>23,24</sup> **Figure 3** illustrates the variation of ionic conductivity as a function of  $1/T(K)$  for the NCPEs having different content of lithium salt and MOF. It can be seen that the ionic conductivity increases with an increase in the MOF content (samples S1 to S4) and a lithium salt content up to 10 wt. %. It begins decreasing with the further increase of lithium salt content (15 wt. %, sample S5). The reduction in



ionic conductivity is attributed to the increase in the viscosity of the polymeric solution.<sup>25,26</sup> The ionic conductivity ranges from  $10^{-8}$  to  $10^{-4}$  S  $\text{cm}^{-1}$  for sample S1 (only PEO+LiTFSI) between 20 and 80 °C. Upon a limited addition of 2 wt. % of Al-BTC MOF in the polymeric matrix, an increase in ionic conductivity nearly of one order of magnitude is observed. However, when both the content of MOF and lithium salt are increased to 10 wt. %, the ionic conductivity is outstandingly increased by more than two orders of magnitude at 20 °C. This happens for sample S4 which has the best ratio between the three active components where optimum conductivity values are achieved. It is worth noting that, according to the DSC results (see Fig. 1), a quite remarkable increase in the  $T_g$  value is observed while adding 10 wt.% of MOF filler content to the PEO+LiTFSI matrix, which normally should reflect in a decrease of the ionic conductivity; curiously, a double fold increase is here evidenced which should be related to some other kind of contribution from the filler and/or specific interactions between the various active components. This is better unravelled in the followings.

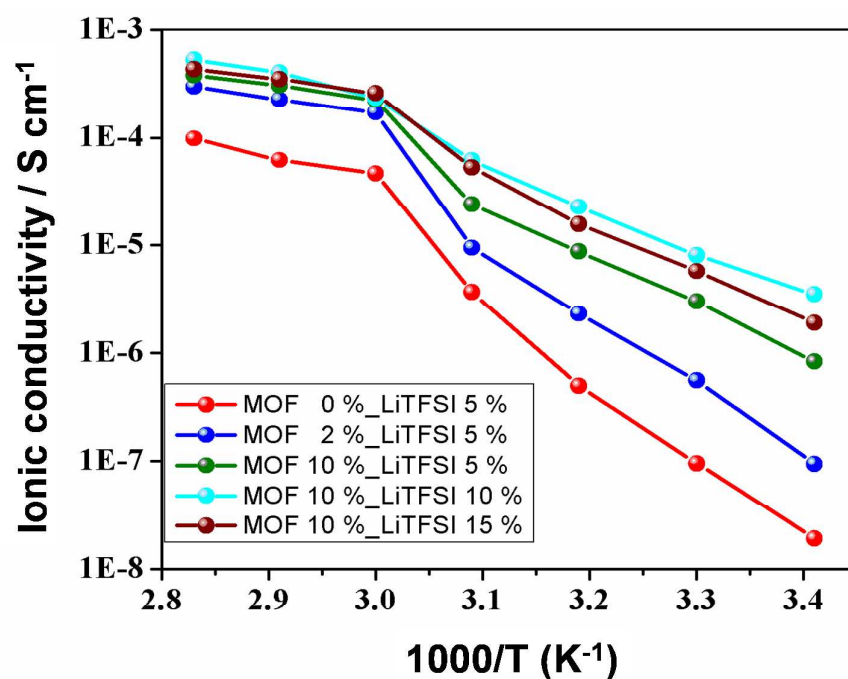


**Fig. 3** Ionic conductivity Arrhenius plot as a function of the temperature (1/K) of the different samples prepared. Data obtained by impedance spectroscopy.

As commonly observed for nanocomposite materials, the ionic conductivity is not a linear function of the filler concentration.<sup>4,5</sup> At low concentration levels, the diffusion effect which tends to depress the conductivity is effectively opposed by the specific interactions of  $\text{Li}^+$  ions with the filler surfaces, this latter effect promoting fast ion transport. Hence, an enhancement in conductivity is observed. On the other hand, at high filler content, the dilution effect predominates and the conductivity decreases.<sup>25</sup> Thus, the maximum conductivity is generally achieved only in the concentration region between 5 and 15 wt. %, chiefly depending on the nature of the filler.<sup>5</sup> According to the NMR studies from Scrosati and co-workers, the local dynamics of the lithium ions, in particular lithium mobility, is not affected by the filler, thus supporting the idea that the enhancement of conductivity by adding a filler is caused by stabilizing and increasing the fraction of amorphous phase.<sup>26</sup> The Lewis acid groups of the added inert filler may compete with the Lewis acid lithium cations for the formation of complexes with the alkoxide of the PEO chains, as well as with the anions of the lithium salt added. Subsequently, this results in structural modifications of the filler surfaces, due to the specific actions of the polar surface groups of the inorganic filler. The Lewis acid–base interaction centres with the electrolytic species, thus lowering the ionic coupling and promotes the salt dissociation via a sort of “ion-filler complex” formation. In the present study, Al-BTC (filler), which has Lewis acid centre, can react with the anions of the lithium salt and these interactions lead to the reduction in the crystallinity of the polymer host (see also Figure 1). Indeed, this effect could be the reason for the observed remarkable enhancement in the ionic conductivity.<sup>15</sup> A deep understanding of the interfacial properties between lithium metal and polymer electrolyte is mandatory in order to provide more insight into the factors controlling the recharge ability of lithium-based polymer batteries. It is well known that the lithium surface is normally almost covered by a passive layer called solid electrolyte interface (SEI) and this layer is believed to play a key role in the electrochemical performance of lithium batteries as far as the calendar life is concerned. Many experimental techniques, such as XPS,<sup>27</sup> infrared spectroscopy,<sup>28</sup> NMR,<sup>29</sup> *in situ* synchrotron X-ray reflectometry,<sup>30</sup> and ellipsometry<sup>31</sup> have been employed to study the nature and

formation mechanism of the SEI layer. Many reasons have been suggested for poor cycling of lithium cells, which include electrochemical reactions between anode and electrolyte and loss of electronic contact between electrode and dendritic lithium. On the other hand, a resistive layer covers the lithium metal electrode in the polymer electrolyte systems and the resistance of this layer grows with time, possibly reaching values over  $10 \text{ k}\Omega \text{ cm}^{-2}$ .<sup>32-33</sup> The nature of this layer depends mainly on the purity and the composition of the electrolyte.

In the present study, the newly elaborated PEO nanocomposite membranes studies were examined in terms of the compatibility (interfacial stability), with proper attention on sample S4, as this composition was found to be optimal from the ionic conductivity point of view. **Figure 4** displays the variation of interfacial resistance,  $R_i$ , as a function of time for the Li/S1(PEO+LiTFSI)/Li and Li/S4-NCPE/Li symmetric cells kept under open circuit condition at  $60^\circ\text{C}$ , which corresponds to the deflection point of the ionic conductivity (see Figure 3) due to the change in the PEO crystallinity.

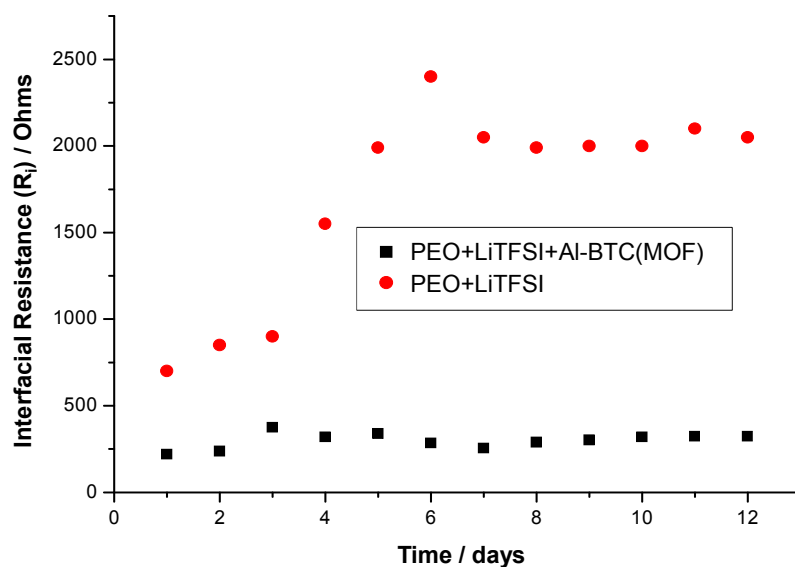


**Fig. 4** Variation of interfacial resistance ( $R_i$ ) as a function of time for the symmetric cells composed of Li/S4-NCPE/Li (black squares) and Li/S1(PEO+LiTFSI)/Li (red dots) both stored at  $60^\circ\text{C}$ .

As described by Abraham and co-workers, the interfacial resistance can be measured from the Cole–Cole impedance plots (see Figure S.10 in S.I.) in which the large semi-circles represent a

parallel combination of resistance ( $R_{\text{film}}$ ) and capacitance associated with the passivation film on the Li metal electrode.<sup>34</sup> A small semicircle is due to the charge transfer resistance in parallel with the double layer capacitance. The intercept of the large semi-circle at high frequency on the Z-axis is mostly associated with the interfacial resistance ( $R_i$ ) of the system. It is observed from the figure that the nanocomposite polymer electrolyte containing the Al-BTC MOF filler is definitively more compatible than the polymer electrolyte prepared by only PEO and LiTFSI, being lithium metal used as the anode. As clearly evident, in the case of sample S4 the resistance values do not change much even after 300 h. This may be explained by assuming that the morphology of the passivation film slightly changes during the initial time to finally acquire a non-compact, possibly porous structure.<sup>35</sup> Furthermore, it is quite obvious from the plot that the overall interfacial resistance of the polymer host is considerably reduced upon the incorporation of the novel nanosized inert filler (much lower than the filler-free membrane). Generally speaking, the nano-sized inert fillers are more compatible than the micron-sized ones. The inert particles, depending upon their volume fraction, would tend to minimize the area of the lithium electrode exposed to polymers containing  $-O-$  and  $-OH$  species, thus reducing the passivation process. It is also foreseeable that small sized particles for a similar volume fraction of the filler (ceramic) phase would impart an improved performance as compared to larger sized particles because they will cover more surface area.<sup>36</sup> The formation of an insulated layer of filler particles at the electrode surface is probable at a higher volume fraction of a passive ceramic phase. This insulating layer will impede electrode reactions. This likely happens in the present system, where 10 wt. % of the MOF filler phase was introduced into the polymer matrix resulting in an homogeneous nanocomposite polymer electrolyte membrane (see the FESEM images of Figure S.8 in S.I.). Moreover, the nanosized MOF particle, as it is based on aluminium based metal has a big affinity towards water. Thus, it can also absorb the impurity that may present in the NCPE to overall improve the stability of the system.

The lithium transference number,  $T_{\text{Li}}^+$ , is a key factor in the optimisation of lithium battery electrolytes. Indeed, high  $T_{\text{Li}}^+$  guarantees high enough power density.<sup>5,6</sup> In our present newly

elaborated nanocomposite polymer system encompassing Al-BTC(MOF), the  $T_{Li^+}$  is 0.55 (see also S.I.), considerably high at moderately low 50 °C temperature which is realistic if one considers the application in hybrid electric transportation.

Multinuclear solid-state NMR analyses and Fourier Transform Infrared Spectroscopy (FT-IR) were used to investigate the possible interactions of MOF with PEO and lithium. The  $^{27}Al$  MAS spectra of the samples Al-BTC(MOF), PEO+Al-BTC(MOF) and PEO+LiTFSI+Al-BTC(MOF) are shown and described in the S.I. (Figure S.12). All the spectra show a main feature at 0 ppm due to aluminium in octahedral coordination, whose right asymmetry is attributed to statistical disorder.<sup>37,38</sup> Two other peaks, accounting for few percent, are observed at 35 and 65 ppm, and can be attributed to aluminium coordinated to five and four oxygen atoms, respectively.<sup>39</sup> These last peaks are likely due to surface defects of the MOF particles and, interestingly, their amount increases in the sample PEO+LiTFSI+Al-BTC(MOF). This is particularly interesting and in accordance with the results from impedance spectroscopy (ionic conductivity previously discussed) and FT-IR analysis (discussed in the followings) which account for defective coordination at some of the sites of the Al-BTC(MOF). **Figure 5** shows the  $^7Li$  MAS spectra of the samples PEO+LiTFSI and PEO+LiTFSI+Al-BTC(MOF). In both cases, the observed spectral lines are in the motionally narrowed regime, which means that the correlation rate for Li motion ( $\tau_c^{-1}$ ) is of the order of the Larmor frequency, and that only the Hamiltonian isotropic contributions are retained. Therefore, the structure observed in the spectrum of PEO+LiTFSI is due to the presence of  $Li^+$  ions in different chemical environments, which are not time-averaged by spin motion during the NMR experiment.<sup>40</sup> Four contributions are found at -0.50, -0.81, -0.97, -1.09 ppm. The addition of MOF caused a substantial narrowing of the line, which assumes a Lorentzian shape (typical of liquid-like motion) with a chemical shift of -0.87 ppm, roughly corresponding to the centre-of-mass of the four contributions previously described. Therefore, the MOF filler is actively participating in plasticising the structure, which is in agreement with the DSC results, and in improving the  $Li^+$  ion mobility. Finally, the  $^{13}C$  CP-MAS spectra of Al-BTC(MOF), PEO+Al-BTC(MOF), PEO+LiTFSI,

and PEO+LiTFSI+Al-BTC(MOF) are shown in S.I. (see Figure S.13). Summarising, from the analysis of the NMR data, it is not possible to clearly unravel the interactions among MOF, polymer and lithium salt, but we may arguably hypothesise that, after the addition of MOF, lithium ions are in a more homogeneous environment, and likely more mobile, compared to the one without MOF.

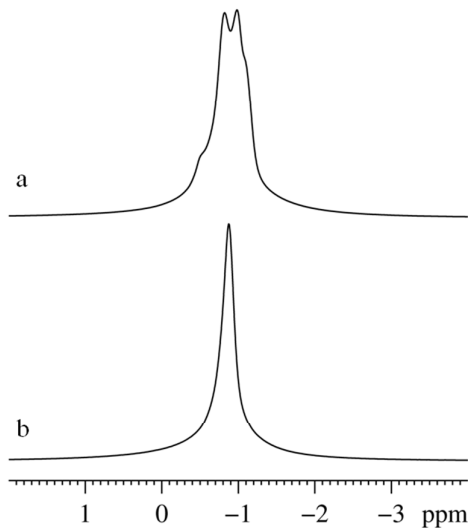


**Fig. 5** Solid state NMR  ${}^7\text{Li}$  MAS spectra a) PEO+LiTFSI, b) PEO+LiTFSI+Al-BTC(MOF). The signal of Li in the PEO+LiTFSI sample is the sum of at least 4 different contributions; addition of Al-BTC(MOF) increases the mobility of  $\text{Li}^+$  ions to which correspond a single NMR peak.

FT-IR was identified as a powerful tool to study the complexation between salts and polymers as it is sensitive to molecular and structural changes in the polymer systems. The FT-IR spectra of PEO, Al-BTC(MOF), PEO+LiTFSI and PEO+LiTFSI+Al-BTC(MOF) are displayed in Figure S.14 and detailed in S.I. In particular, we may observe that the strongest peak of PEO, C–O–C at  $1104\text{ cm}^{-1}$ , is shifted to  $1106\text{ cm}^{-1}$  in the complex upon incorporation of LiTFSI. The intensity of the peak is further reduced when both Al-BTC(MOF) and LiTFSI are laden together in the polymeric matrix. The reduction in the intensity of the peak may be ascribed to the complex formation between PEO, Al-BTC(MOF) and LiTFSI. In a similar way, a reduction in the peak is observed for  $-\text{CH}_2-$  twisting at  $955\text{ cm}^{-1}$  and C–H stretching band centred around  $2900\text{ cm}^{-1}$ . A similar behaviour has been already observed in previous works where the interaction between PEO and lithium salts along

with chitin filler have been demonstrated.<sup>22,41</sup> As for the aforementioned NMR data, FT-IR analysis confirms the presence of some non-coordinated defective Al centres which, in turn, indicates that not all carboxylic groups are deprotonated. Even though no direct evidences are available, the lithium ions may interact with these comparatively stronger free carboxylic groups in the NCPE thus resulting in an improved mobility. This result is also in accordance with the shift observed in the XPS data shown in Figure S.11 in S.I. These –COOH groups present in the Al-BTC(MOF) could be also one of the reasons for the amorphous characteristics of the synthesised metal organic framework which can be also related to the increased ionic mobility with respect to a perfectly crystalline framework.

In order to demonstrate the feasibility of the novel Al-BTC(MOF)-laden PEO-based electrolytes, sample S4 was assembled in a lab-scale lithium cell, sandwiched between a LiFePO<sub>4</sub>/C nanocomposite cathode and a lithium metal anode and its electrochemical behaviour tested at different temperatures and different current rates upon long-term cycling. Compared with conventional layered cathode materials based on transition metal oxides widely used in Li-ion batteries, LiFePO<sub>4</sub> was chosen due to its unique properties such as thermal stability, non-toxicity, eco-friendliness, cost-effectiveness and easy preparative methods.<sup>42</sup> Moreover, it was identified as the ultimate choice as cathode material for nanocomposite polymer electrolyte systems, showing a flat operating voltage of 3.45 V vs. Li and good discharge capacity at low C-rates. In particular, we decided to show the results obtained by using a hydrothermally synthesized LiFePO<sub>4</sub> developed in our Labs, because of the ready availability and the overall reasonably good performances.<sup>42</sup>

The results of the galvanostatic charge/discharge cycling in lab-scale lithium cell are plotted in **Figure 6(a-c)**. It shows typical charge and discharge profiles vs. specific capacity at 1C rate and 70 °C (plot a), the specific capacity as a function of the cycle number at 70 °C and different current regimes from C/10 to 5C (plot b) and the specific capacity as a function of the cycle number at 1C rate and different temperatures (plot c). The cell operates with the expected potential profiles: typical charge and discharge potential versus time profiles between 3.0 and 3.8 V vs. Li at 1C rate

show highly reproducible and well defined plateaus at about 3.48 V vs. Li upon charge (delithiation) and about 3.37 V vs. Li upon discharge (lithiation), which are well in agreement with the characteristic behaviour of LiFePO<sub>4</sub> electrodes upon reversible redox reaction with lithium. The cell demonstrates a specific capacity exceeding 135 mAh g<sup>-1</sup> during the initial cycles at low C/10 but, in particular, the capacity retention while increasing the current regime is definitely remarkable: specific capacity values of about 131, 125 and 118 mAh g<sup>-1</sup> are obtained at C/5, C/2 and 1C rates, respectively, that is almost 88 % capacity retention from C/10 to 1C after about 80 complete cycles. The results are clearly at the level of the performances obtained with the same LiFePO<sub>4</sub>-based cathode in standard liquid electrolyte cell described in Meligrana et al.,<sup>42</sup> thus accounting for the remarkable characteristics of the newly elaborated Al-BTC(MOF)-laden PEO-based electrolyte. The cell demonstrates a stable behaviour at each of the tested currents and can deliver specific capacity approaching 100 mAh g<sup>-1</sup> after 100 cycles at reasonably high 2C rate. In addition, the Coulombic efficiency rapidly increases to above 98% after the first cycles and remains highly stable throughout the cycles (even approaching 100 % at high current regimes), so indicating good mechanical stability of the electrode during the Li<sup>+</sup> ions intercalation/deintercalation process, good interfacial contact and charge transport between the electrodes and the polymer electrolyte, and excellent reversible cycling after the initial surface reactions are complete. The cell is still able to operate at a specific capacity of 40 mAh g<sup>-1</sup> even at 5C rate; which accounts for the remarkable characteristics of the all-solid electrolyte which facilitates the fast lithium ion exchange between the electrodes through the polymer matrix.

Finally, it is important to note that the system behaviour remains correct after prolonged cycling at high regimes, with no abnormal drift: in fact, reducing the rate to 1C almost completely restores the specific capacity (< 5 % decay when comparing the specific capacity values of cycle 70 and 150 at the same 1C rate).



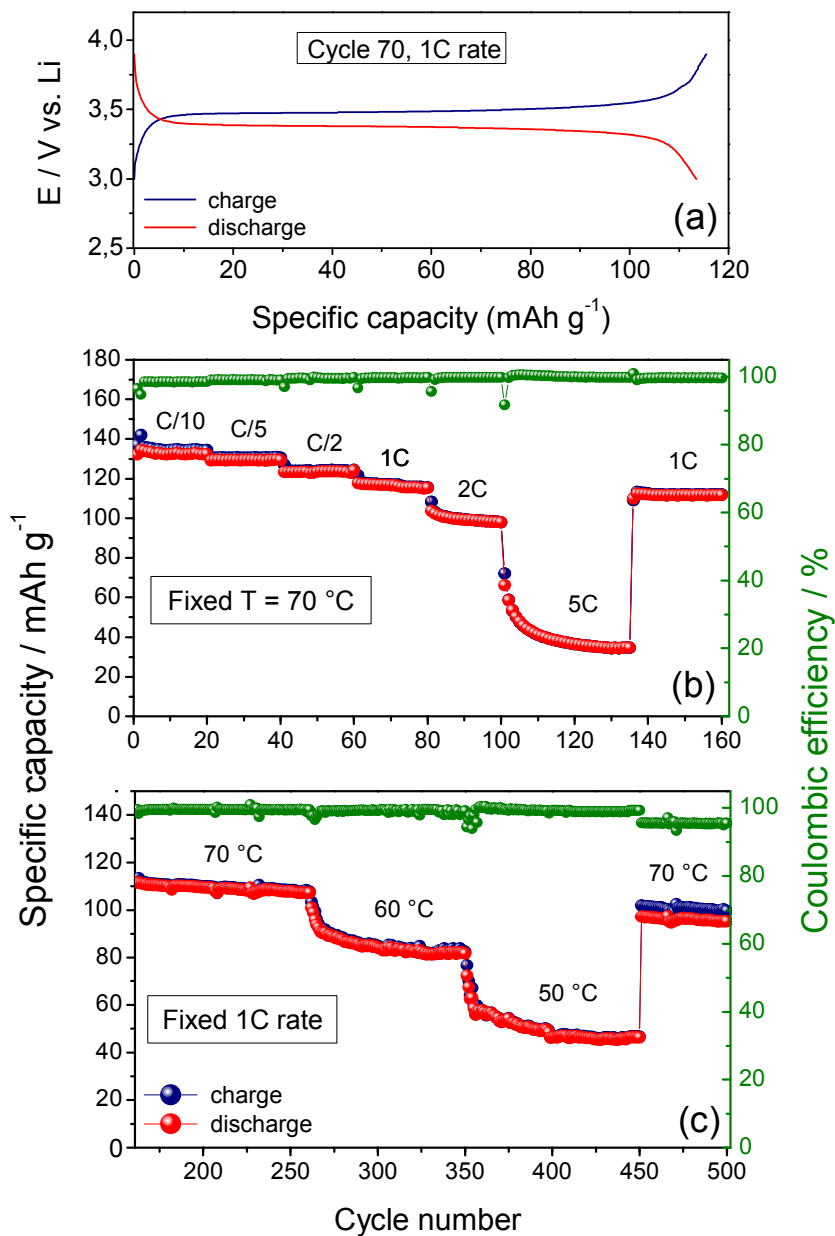


**Fig. 6** Electrochemical characteristics of the  $\text{LiFePO}_4/\text{S4-NCPE}/\text{Li}$  cell at different temperatures and current regimes. a) Typical potential vs. time profiles at  $70\text{ }^\circ\text{C}$  and  $1\text{C}$  rate; b) galvanostatic discharge/charge cycling test at fixed  $70\text{ }^\circ\text{C}$  and varying C-rates (from  $\text{C}/10$  to  $5\text{C}$ ) along with the Coulombic efficiency; c) prolonged galvanostatic cycling at fixed  $1\text{C}$  rate and varying temperatures along with the Coulombic efficiency.

After the initial 160 cycles at fixed  $70\text{ }^\circ\text{C}$  and different C-rates were completed, the positive electrochemical characteristics of fully-solid lithium cell comprising the newly elaborated NCPE upon reversible reaction with lithium were confirmed by prolonging the charge/discharge test for very long-term cycling (from 160 to 500 cycles), by fixing the same  $1\text{C}$  rate and modulating the

temperature. The results are shown in plot (c) of Figure 6. The specific capacity of the cell is significantly reduced when reducing the temperature, as for the decrease in the ionic conductivity of the nanocomposite polymer electrolyte. Nonetheless, a stable cycling profile is achieved even at 50 °C, with a reversible specific capacity of about 45 mAh g<sup>-1</sup>, which has never been reported so far for an all solid-state lithium polymer cell composed of Li/NCPE/LiFePO<sub>4</sub>. After restoring the temperature back to 70 °C, the decay in specific capacity of the cell is found to be limited (around 12 % decay when comparing the specific capacity values of cycle 250 and 450 at the same 70 °C) and the cell is able to operate at its initial capacity even after 500 cycles, with a slight decrease in Coulombic efficiency. Overall, the highly stable cycling performance with good capacity retention proves that the novel nanocomposite polymer electrolyte PEO+LiTFSI+Al-MOF can be a good candidate for all solid state lithium batteries conceived for moderate temperature applications.

In conclusion, we presented here the successful dispersion of an aluminium-based metal-organic framework (Al-BTC MOF) in a PEO-based polymer matrix, thus producing high performing polymer electrolytes for Li-based batteries. Besides the very interesting thermal and long-term stable interfacial characteristics, a two orders of magnitude enhancement in the ambient temperature ionic conductivity of poly(ethylene oxide)-based nanocomposite polymer electrolyte (NCPE) membranes was demonstrated for the first time by the incorporation of specific amounts of the Al-BTC(MOF) filler. An excellent cycling profile was achieved, stable even at 50 °C, with the newly elaborated, sustainable all solid state lithium polymer cell composed of Li/NCPE/LiFePO<sub>4</sub>. The strategic effect achieved by the optimal combination of the active components employed in the NCPE preparation opens up new and interesting prospects in the design of thinner, safer, sustainable and higher performing all-solid-state energy storage devices with outstanding characteristics of durability and rate capability even at moderately low temperatures.

**Acknowledgements:** One of the authors (A.M.S.) gratefully acknowledges CSIR, New Delhi for the financial support to visit Politecnico di Torino (Italy) under Raman Research Fellowship. The

authors would like to thank Mr. Mauro Raimondo for the FESEM/STEM analysis and Dr. Salvatore Guastella for the XPS analysis. Dr. Sonia Lucia Fiorilli, Dr. Nadia Garino, Dr. Stefania Ferrari and Mr. Federico Bella are gratefully acknowledged for the support.

## References

- [1] P.G. Bruce, B. Scrosati, J.-M. Tarascon, *Angew. Chem. Int. Ed.*, 2008, **4**, 2930.
- [2] J.-M. Tarascon, M. Armand, *Nature*, 2001, **414**, 359.
- [3] A. Guerfi, M. Dontigny, Y. Kobayashi, K. Zaghib, *J. Sol. State Electrochem.*, 2009, **13**, 1003.
- [4] A. Manuel Stephan, *Europ. Polym. J.*, 2006, **42**, 21.
- [5] E. Quartarone, P. Mustarelli, *Chem. Soc. Rev.*, 2011, **40**, 2525.
- [6] B. Scrosati, *Chem. Rec.*, 2005, **5**, 286.
- [7] J.E. Weston, B.C.H. Steele, *Solid State Ionics*, 1982, **7**, 75.
- [8] F. Croce, G. B. Appetecchi, L. Persi, B. Scrosati, *Nature*, 1998, **394**, 456.
- [9] a) F. Croce, R. Curini, A. Martinelli, L. Persi, F. Ronci, B. Scrosati, *J. Phys. Chem. B*, 1999, **103**, 10632; b) C. Capiglia, P. Mustarelli, E. Quartarone, C. Tomasi, A. Magistris, *Solid State Ionics*, 1999, **118**, 73.
- [10] F. Croce, L. Settini, B. Scrosati, *Electrochem. Commun.*, 2006, **8**, 364.
- [11] Z. Gadjourova, Y. Andreev, D.P. Tunstall, P.G. Bruce, *Nature*, 2001, **412**, 148.
- [12] a) M. Eddaoudi, H. Li, O.M. Yaghi, *J. Am. Chem. Soc.*, 2000, **122**, 1391; b) D. Saha, R. Zacharia, L. Lafi, D. Cossement, R. Chahine, *Chem. Eng. J.*, 2011, **171**, 517.
- [13] F. Bella, R. Bongiovanni, R.S. Kumar, M.A. Kulandainathan, A.M. Stephan, *J. Mater. Chem A*, 2013, **1**, 9033.
- [14] a) A. Dhakshinamoorthy, M. Alvaro, H. Garcia, *Chem. Commun.*, 2012, **48**, 11275; b) H. Hosseini, H. Ahmar, A. Dehghani, A. Bagheri, A. Tadjarodi, A.R. Fakhari, *Biosens. Bioelectron.*, 2013, **42**, 426; c) C. Chen, J. Kim, D.A. Yang, W.S. Ahn, *Chem. Eng. J.*, 2011, **168**, 1134; d) J.

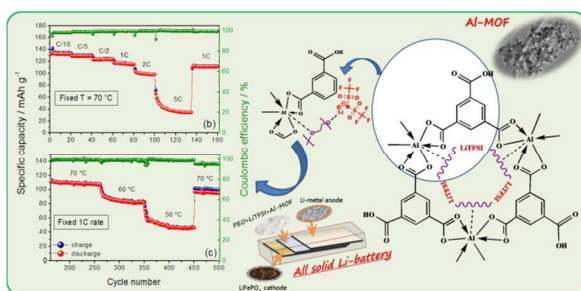
- Yang, A. Grzech, F.M. Mulder, T.J. Dingemans, *Microp. Mesop. Mater.*, 2013, **171**, 65; e) M. Fischer, F. Hoffmann, M. Fröba, *RSC Adv.* 2012, **2**, 4382; f) J.R. Li, J. Sculley, H.C. Zhou, *Chem. Rev.*, 2012, **112**, 869; g) R.S. Kumar, S.S. Kumar, M.A. Kulandainathan, *Electrochem. Commun.*, 2012, **25**, 70.
- [15] B.M. Wiers, M.-L. Foo, N.P. Balsara, J.R. Long, *J. Am. Chem. Soc.*, 2011, **133**, 14522.
- [16] C. Yuan, J. Li, P. Han, Y. Lai, Z. Zhang, J. Liu, *J. Power Sources*, 2013, **240**, 653.
- [17] G.B. Appetecchi, J. Hassoun, B. Scrosati, F. Croce, F. Cassel, M. Salomon, *J. Power Sources*, 2003, **124**, 246.
- [18] Z. Guo, Z. Fang, L. Tong, Z. Xu, *Polym. Degrad. Stabil.*, 2007, **92**, 545.
- [19] S.P. Thomas, S. Thomas, S. Bandyopadhyay, *J. Phys. Chem. C*, 2009, **113**, 97.
- [20] R. Ribeiro, G.G. Silva, N.D.S. Mohallen, *Electrochim. Acta*, 2001, **46**, 1679.
- [21] T. Shodai, B.B. Owens, M. Ohtsuka, J. Yamaki, *J. Electrochem. Soc.*, 1994, **141**, 2978.
- [22] A. Manuel Stephan, T.P. Kumar, M. Anbu Kulandainathan, N. Angulakshmi, *J. Phys. Chem. B*, 2009, **113**, 1963.
- [23] K. Xu, *Chem. Rev.*, 2004, **104**, 4303.
- [24] K. Matsumoto, K. Inoue, K. Nakahara, R. Yuge, T. Noguchi, K. Utsugi, *J. Power Sources*, 2013, **231**, 234.
- [25] W. Wiczoreck, J.R. Steven, Z. Florjanczyk, *Solid State Ionics*, 1996, **85**, 67.
- [26] F. Croce, L. Persi, B. Scrosati, F. Serraino-Fiory, E. Plichta, M.A. Hendrickson, *Electrochim. Acta*, 2001, **46**, 2457.
- [27] F.M.S. Wu, P.C.J. Chiang, J.C. Lin, *J. Electrochem. Soc.*, 2005, **152**, A1041.
- [28] G.D. Aurbach, K. Gamolsky, B. Markovsky, G. Salitra, Y. Gofer, U. Heider, R. Oesten, M. Schmidt, *J. Electrochem. Soc.*, 2000, **147**, 1322.
- [29] H.M. Menetrier, C. Vaysse, L. Croguennec, C. Delmas, C. Jordy, F. Bonhomme, P. Biensan, *Electrochem. Solid State Lett.*, 2004, **7**, A140.

- [30] I.M. Hirayama, N. Sonoyama, T. Abe, M. Minoura, M. Ito, D. Mori, A. Yamada, R. Kanno, T. Terashima, M. Takano, K. Tamura, J. Mizuki, *J. Power Sources*, 2007, **168**, 493.
- [31] J.L. Lei, L.J. Li, R. Kostecki, R. Muller, F. McLarnon, *J. Electrochem. Soc.*, 2005, **152**, A774.
- [32] C.D. Robitaille, D. Fauteux, *J. Electrochem. Soc.*, 1986, **133**, 315.
- [33] D. Aurbach, I. Weissman, H. Yamin, E. Elster, *J. Electrochem. Soc.*, 1998, **145**, 1421.
- [34] Z. Jiang, B. Carroll, K.M. Abraham, *Electrochim. Acta*, 1997, **42**, 2667.
- [35] G.B. Appetecchi, F. Croce, B. Scrosati, *Electrochim. Acta*, 1995, **40**, 991.
- [36] A. Manuel Stephan, K.S. Nahm, T. Prem Kumar, M. Anbu Kulandainathan, G. Ravi, J. Wilson, *J. Power Sources*, 2006, **159**, 1316.
- [37] C. Leonelli, G. Lusvardi, M. Montorsi, M. C. Menziani, L. Menabue, P. Mustarelli, L. Linati, *J. Phys. Chem. B*, 2001, **105**, 919.
- [38] D.R. Neuville, L. Cormier, D. Massiot, *Geochim. Cosmochim. Acta*, 2004, **68**, 5071.
- [39] S. Risbud, R.G. Kirkpatrick, A. Tagliavere, B. Montez, *J. Am. Ceram. Soc.*, 1987, **70**, C10.
- [40] P. Mustarelli, C. Capiglia, E. Quartarone, C. Tomasi, P. Ferloni, L. Linati, *Phys. Rev. B*, 1999, **60**, 7228.
- [41] N. Angulakshmi, T. Prem Kumar, S. Thomas, A. Manuel Stephan, *Electrochim. Acta*, 2010, **55**, 1401.
- [42] G. Meligrana, C. Gerbaldi, A. Tuel, S. Bodoardo, N. Penazzi, *J. Power Sources*, 2006, **160**, 516.

**Table of Content (TOC) entry**

*Innovative high performing metal organic framework (MOF)-laden nanocomposite polymer electrolytes for all-solid-state lithium batteries*

Claudio Gerbaldi, Jijeesh R. Nair, M. Anbu Kulandainathan, R. Senthil Kumar, Chiara Ferrara, Piercarlo Mustarelli and Arul Manuel Stephan



Al-based metal organic framework (MOF): novel nanofiller for polymer electrolytes with outstanding moderate temperature ionic conductivity and long-term cycling stability.